Parent material and climate interact to control soil C dynamics through the development of poorly crystalline minerals

Jeffrey Beem-Miller[1], Craig Rasmussen[2], Alison M. Hoyt[1,3], Marion Schrumpf[1], Georg Guggenberger[4], & Susan Trumbore[1]

[1] Department of Biogeochemical Processes, Max Planck Institute for Biogeochemistry, Jena, Germany

[2] Department of Environmental Science, The University of Arizona, Tucson, AZ, USA

[3] Department of Earth System Science Science, Stanford University, Stanford, CA, USA

[4] Institute of Soil Science, Leibniz University Hannover, Hannover, Germany

Abstract

Lorem ipsum...

Parent material and climate interact to control soil C dynamics through the development of poorly crystalline minerals

Key messages:

- Climate explains more variance in $\Delta^{14}C$ at the soil surface; parent material explains more variance at depth
- Interaction of parent material and climate explains more variance in bulk soil and respired $\Delta^{14}C$ than either factor alone
- Poorly crystalline mineral content is highly correlated with the difference between bulk soil and respired $\Delta^{14}C$

Introduction

Climate change will determine whether or not soils will continue to be a sink for atmospheric carbon or become a source in the coming decades. Understanding the response of soil carbon to these changes requires insight into the mechanisms of soil carbon protection. In this study we considered the relative effects of parent material and climate on the distribution of radiocarbon in bulk soils and heterotrophically respired CO_2 in order to determine how these factors control the cycling of soil C across timescales of years to centuries.

Climate, and in particular temperature, has been found to be the most important variable aside from depth for explaining the distribution of ages of soil carbon at a global scale. Yet our current understanding of soil organic matter decomposition underscores the importance of physical mechanisms that may attenuate the classical temperature-decomposition relationship. Among the most salient of these mechanisms is the association of soil organic matter with minerals.

Soil mineral assemblages are the result of the weathering of primary minerals to form secondary minerals, and the preferential loss or stabilization of those secondary minerals over time. Differences in climate can therefore lead to different soil mineral assemblages when starting from the same parent materials, or to similar mineral assemblages despite starting from disparate parent materials. The relevance of soil minerals for mediating soil organic matter protection appears to be a function of the specific minerals present, rather than the amount of clay or total mineral surface area (Beyond Clay, etc.).

The soils in the current study comprise a parent material (granite, andesite, basalt) by climate gradient (warm, cool, cold), but also a weathering gradient in tandem with climate. The high elevation, cold climate soils (MAT = 5.5°C) in this study are poorly developed, while the cool climate soils (MAT = 9°C) are in intermediate stages of weathering, and the warm climate soils (MAT = 11.5°C) are highly weathered. Previous research characterizing the mineral assemblages at these sites using XRD and selective dissolution found that the dominant mineral species in the soils of the most weathered warm climate zone were similar across parent materials, and consisted of 1:1 clays with large accumulations of crystalline iron oxides. In contrast to the warm climate sites, mineral assemblages at the cool and cold climate sites differed substantially. The andesitic soils are characterized by large amounts of short-range order (SRO) minerals such as allophane and iron oxyhydroxides, while the basaltic soils have intermediate amounts of SRO minerals and the granitic soils lack SRO minerals almost entirely, but have relatively more hydroxyl-interlayered vermiculite.

The strength and sorptive capacity of soil minerals is dependent not only on the available surface area of soil minerals, but also on the potential for ligand exchange, which is a function of the density of accessible hydroxyl groups (Kaiser and Guggenberger, 2003; Rasmussen et al., 2018 “Beyond Clay”; Kleber et al., 2015). Pedogenic oxides are particularly enriched in hydroxyl groups, and batch sorption/desorption experiments have shown that the mineral-organic interactions between pedogenic oxide rich clays are stronger

than those with siloxane-rich phyllosilicate clays (Kahle et al., 2004). Furthermore, the reactive properties of pedogenic oxides can also facilitate lower strength interactions with soil organic matter through multivalent cation bridging (Kleber et al., 2007). The importance of pedogenic oxides for explaining both soil C concentration and bulk soil radiocarbon ($\Delta^{14}C_{bulk}$) is confirmed for our study sites by the findings of Rasmussen et al. (Soil systems, 2018), who observed that oxalate extractable iron was the best predictor of both properties. However, the relevance of mineral-organic associations with either pedogenic oxides or 1:1 clays for explaining the dynamics of more transiently cycling soil C is poorly studied.

Radiocarbon (^{14}C) is a useful tracer for soil C dynamics over time scales ranging from annual to millennial. The use of ^{14}C to measure timescale of soil carbon decomposition relies on our knowledge of the ratio of $^{12}C/^{14}C$ in the atmosphere. Once CO_2 is fixed into organic matter via photosynthesis, this ratio starts to shift as 14C is preferentially lost due to radioactive decay. Changes in the $^{12}C/^{14}C$ ratio due to radioactive decay are detectable at the relatively longer timescales of hundreds to thousands of years. However, we can detect changes in ^{14}C with nearly annual resolution for the so-called "bomb-C" period, which began with the deployment and atmospheric testing of nuclear weapons in the mid-20^{th} century. This pulse of "bomb-C" led to a 2-fold increase in the concentration of 14C in the atmosphere before testing was banned in 1963. However, the level of ^{14}C in the atmosphere returned to pre-bomb levels around 2020, meaning that archived samples now represent the best opportunity for taking advantage of the bomb-C pulse.

Soil is an open system, and this has important implications for the interpretation of radiocarbon measurements of soil C. For most soils, the majority of carbon that enters the soil leaves relatively quickly, with only a small fraction persisting (Sierra et al. 2018). Accordingly, in order to assign an age to soil C from radiocarbon measurements it is necessary to construct a model of inputs, outputs, and potential transfers of C among different pools in the soil that may be more or less protected from decomposition (Sierra et

al., 2017). Our current understanding of soil C persistence points to the association of soil organic matter with minerals, the occlusion of soil organic matter within aggregates, and chemical recalcitrance of soil organic matter as the most important mechanisms for protecting soil C from decomposition (Lehmann and Kleber, 2015).

Radiocarbon measurements of bulk soil C typically capture the signal from persistent pools, while more transient pools dominate measurements of C leaving the soil via heterotrophic respiration (Trumbore 2000). For any given soil, the distribution of soil C among pools with different degrees of persistence will determine the mean age, while the relative contribution of these different pools to respiration will determine the transit time, or the average amount of time spent in the soil by a given atom of C (Sierra et al. 2017). If the radiocarbon measurements of $\Delta^{14}C_{bulk}$ and heterotrophically respired CO_2 ($\Delta^{14}C_{respired}$) are the same, it indicates that the soil lacks substantial protective mechanisms and that all of the C in the soil has an equal probability of being decomposed by microbes. When $\Delta^{14}C_{bulk}$ and $\Delta^{14}C_{respired}$ are substantially different, however, this can be taken as evidence for the presence of persistent pools of soil C.

In the following study we will show that both climate and parent material are important factors for explaining the distribution of $\Delta^{14}C_{bulk}$ and $\Delta^{14}C_{respired}$. Furthermore, we will demonstrate that in order to explain the variation we observe in $\Delta^{14}C_{bulk}$ and $\Delta^{14}C_{respired}$ we must consider the interaction of parent material and climate via weathering. This interaction can be quantified via characterization of the mineral assemblages present in the soil, and we will show how the presence of poorly crystalline minerals is key for explaining not only $\Delta^{14}C_{bulk}$, but also the relationship between $\Delta^{14}C_{respired}$ and $\Delta^{14}C_{bulk}$. In particular, we provide novel evidence for the importance of mineral associations in determining the relative contribution of persistent soil C pools to respiration. Finally, through the quantification of poorly crystalline and crystalline minerals we show how weathering of different parent materials leads to both similarities and differences in mineral

assemblages, and critically, how these mineral assemblages affect the response of soil C dynamics to different climate regimes over timescales ranging from years to centuries.

Methods

Site descriptions

We collected samples from 9 sites across a combined gradient of parent material and climate in the Sierra Nevada Mountains of California (**Fig. 1**). These mountains provide natural independent gradients of parent material and climate. Moving from north to south along the cordillera the parent material changes from basalt to andesite to granite, while the change in elevation headed eastward from the Central Valley leads to a decrease in mean annual temperature (MAT) that is consistent for each parent material.

Total mean annual precipitation is relatively constant with elevation, but falls mainly as rain at lower elevations, and mainly as snow at higher elevations. There is a slight precipitation gradient running north to south, with MAP of xxx mm yr^{-1} averaged across the basalt sites in the north, xxx mm yr-1 for the andesitic sites, and xxx mm yr^{-1} for the granodiorite sites in the south (**Fig. 1**).

Vegetation at the study sites is typical of the Sierra Mixed Conifer habitat (Parker, I., and W. J. Matyas. 1981. CALVEG: a classification of Californian vegetation. U.S. Dep. Agric., For. Serv., Reg. Ecol. Group, San Francisco.). All of the sites are forested and dominated by conifers, although the species composition changes along with climate. Tree species at the lowest elevation, "warm", sites are predominantly *Pinus ponderosa* mixed with lesser amounts of *Quercus* spp. The canopy species at the mid-elevation "cool" sites are comprised primarily of *Abies concolor* and *Pinus lambertiana*, while *Abies magnifica* is the dominant species at the highest elevation "cold" sites. Species present at all sites include

Calocedrus decurrens in the canopy, the shrubs *Arctostaphylos* spp., *Chamaebatia foliolosa*, and *Ceanothus* spp. to varying degrees, and ground cover of grasses and forbs (**Fig. 1**).

Ecosystem	Dominant Vegetation	Elevation (m a.s.l.)	MAP (mm yr^{-1})	MAT (°C)	Parent Material	Soil Taxonomy
PP	*Pinus ponderosa*	920–1400	80–130	10–13	GR	fine-loamy, mixed, semiactive, mesic Ultic Haploxeralf
	Pinus lambertiana		Mostly rain		BS	fine, kaolinitic, mesic Xeric Haplohumult
	Quercus kelloggii				AN	fine, parasesquic, mesic Andic Palehumult
WF	*Abies concolor*	1500–1800	80–130	8–10	GR	coarse-loamy, mixed, superactive, mesic Humic Dystroxerept
	Pinus ponderosa		Rain/snow		BS	loamy-skeletal, mixed, superactive, mesic Typic Haploxerept
	Pinus lambertiana				AN	medial-skeletal, amorphic, mesic Humic Haploxerand
RF	*Abies magnifica*	2200–2400	100–130	5–6	GR	mixed, superactive, frigid Dystric Xeropsamment
	Pinus jeffreyi		snow		BS	sandy-skeletal, mixed, superactive, frigid Typic Xerorthent
					AN	medial-skeletal, amorphic, frigid Humic Vitrixerand

Figure 1. NB: this is a placeholder—copied verbatim from Rasmussen et al. 2018 Dominant vegetation, climate parameters, and soil taxonomy for sampled ecosystems.[1] MAP—mean annual precipitation; MAT—Ecosystem abbreviations: PP—ponderosa pine; WF—white fir; RF—red fir. Dominant vegetation is listed in order of over-story dominance. Parent material abbreviations: GR—granite; BS—basalt; AN—andesite.

Sample collection

Site locations were initially established in 2001 by C. Rasmussen (Rasmussen et al., 2006), and resampled in 2009 (Rasmussen et al., 2018). We returned in late September of 2019 to collect samples for a third timepoint. Sites were located using GPS and geospatial coordinates recorded during site establishment. At each site we dug three replicate pits down

to a depth of 0.3m. Prior to sample collection we compared the soil profiles to the pedon descriptions from the previous sampling campaigns. After confirming profiles were comparable we collected samples from the pit sidewalls in 0.1m increments for each of the three pits. We also measured the depth of the litter layer and collected representative litter samples from each site.

Spline fitting

Soils collected in 2001 and 2009 were sampled by horizon, while soils collected in 2019 were sampled by depth. We were motivated to use consistent depth increments across sites because of the strong correlation between depth and $\Delta^{14}C$. In order to make the horizon and depth-based measurements comparable, we fit a mass-preserving quadratic spline to the 2001 and 2009 profiles in order to convert soil property data to the equivalent depth increments sampled in 2019 (Bishop et al., 2001). We used the mpspline function of the GSIF package in R, with a lamba value of 0.1 (Hengl 2019).

Incubations

Laboratory soil incubations were performed on composite samples from the three replicate pedons sampled at each site. We composited and incubated each depth increment (0-10 cm, 10-20 cm, 20-30 cm) separately in 1 L glass mason jars fitted with sampling ports in the lids. Incubations were performed in duplicate. Prior to the start of incubations we adjusted the soil moisture content to 60% of water holding capacity (WHC). We defined WHC as the gravimetric water content of water-saturated soil placed in mesh-covered (50µm) tubes (50ml) weighed after draining for 30 minutes on a bed of fine sand. Following rewetting we allowed the soils to respire for one week before closing the jars. Incubations proceeded until CO_2 concentrations in the jar headspace reached approximately 10,000 ppm,

at which point we collected a 400ml gas subsample for radicocarbon analysis. Gas samples were collected with pre-evacuated stainless-steel (Restec) vacuum canisters. All incubations were performed in the dark at 20°C.

Soil Physical Analyses and Mineral Characterization

Data on soil particle size distributions, bulk density, and mineral characterization were obtained from previously published analyses of samples collected at the study sites in 2001 and 2009 (Rasmussen et al. 2006, Rasmussen et al., 2018). Both qualitative and quantitative approaches were used to characterize soil mineral assemblages, including X-ray diffraction (XRD) for the clay (<2µm) fraction, atomic absorption spectroscopy, and non-sequential selective dissolution. Details on these analyses are provided by Rasmussen et al. (20XX). In this study we use the sum of ammonium-oxalate extractable aluminum and half of the ammonium-oxalate extractable iron selectively dissolved from bulk soils as a proxy for the abundance of poorly and non-crystalline minerals, and the difference of dithionite-citrate extractable iron and ammonium-oxalate extractable iron for the abundance of crystalline minerals.

Carbon, Nitrogen, and Radiocarbon Analysis

Total carbon and nitrogen content was determined by dry combustion (Vario Max, Elementar Analysensysteme GmbH) on finely ground soils (Retch MM400). For radiocarbon analysis, we first purified CO_2 from incubation flask samples and combusted soil samples on a vacuum line using liquid N_2. Following purification, samples were graphitized with an iron catalyst under an H_2 enriched atmosphere at 550°C. Radiocarbon content was then measured by accelerator mass spectrometry (Micadas, Ionplus, Switzerland) at the Max Planck Institute for Biogeochemisty (Steinhof, 2017).

We report radiocarbon values using units of Δ^{14}C, defined as the deviation in parts per thousand of the ratio of ^{14}C–^{12}C from that of the oxalic acid standard measured in 1950. This unit also contains a correction for the potential effect of mass-dependent fractionation by normalizing sample δ^{13}C to a common δ^{13}C value of 25 per mil (Stuiver & Polach, 1977). Values with Δ^{14}C >0 indicate the presence of "bomb" C produced by atmospheric weapons testing in the early 1960s. Values with $\Delta^{14}C < 0$ indicate the influence of radioactive decay of ^{14}C, which has a half-life 5730 years.

Statistical analysis

We used a linear modeling approach to assess the relative explanatory power of climate versus parent material on the observed variation in Δ^{14}C, as well as potential interactions between these two factors. We constructed separate models for $\Delta^{14}C_{bulk}$ and $\Delta^{14}C_{respired}$ but with the same righthand side of the equation. For each model we considered the two-way interaction between parent material and climate as well as the three-way interaction with time (**Eq. 1**). For ease of interpretation, we considered the effect of depth by modeling each depth layer separately (0-10 cm, 10-20 cm, 20-30 cm). We also made pairwise comparisons of $\Delta^{14}C_{bulk}$ and $\Delta^{14}C_{respired}$ across sites and within years, as well as comparisons of individual sites across years. We assessed the significance of the temporal trend for pairwise combinations of parent material and climate using the emmtrends function of the emmeans package (Lenth, 2021). We corrected for multiple comparisons using Tukey's honestly significant mean difference.

Eq. 1

$$\Delta^{14}C = \alpha + \beta_1(Parent\_material) \times \beta_2(Climate) \times \beta_3(Year) + \epsilon$$

The relationship between Δ^{14}C of bulk soil and respired CO_2 provides insight into soil C dynamics and potential retention mechanisms (Sierra et al. 2018). We modeled the effects of

parent material (**Eq. 2**) and climate (**Eq. 3**) on this relationship separately, as we did not have an adequate number of observations to consider the interaction between these two explanatory variables. We used Δ^{14}C measurements made on samples collected in 2001 and 2019, and data from all depths. The three-way interactions of $\Delta^{14}C_{bulk}$ and the explanatory variables were not significant with either depth or time for either **Eq. 3** or **Eq. 4**, so we did not include those variables in the models.

Eq. 2

$$\Delta^{14}C_{respired} = \alpha + \beta_1(\Delta^{14}C_{bulk}) \times \beta_2(Parent\_material) + \epsilon$$

Eq. 3

$$\Delta^{14}C_{respired} = \alpha + \beta_1(\Delta^{14}C_{bulk}) \times \beta_2(Climate) + \epsilon$$

We assessed the relative importance of poorly crystalline versus crystalline iron minerals in protecting soil C from microbial decomposition by regressing Δ^{14}C against the concentrations of ammonium-oxalate extractable iron, ammonium-oxalate extractable aluminum, pyrophosphate extractable aluminum, and dithionite-citrate extractable iron (**Eq. 4**). We fit the model for $\Delta^{14}C_{bulk}$, $\Delta^{14}C_{respired}$, and the difference between $\Delta^{14}C_{respired}$ and $\Delta^{14}C_{bulk}$ ($\Delta^{14}C_{bulk\text{-}respired}$). We used Δ^{14}C data from 2001 and 2019. Selective dissolution was only performed for the soils collected in 2001, however, as these data reflect weathering processes that operate timescales beyond the 18 year duration of this study. We conducted regressions for the entire 0-30 cm depth as extracted metal concentrations did not change substantially by horizon, and this approach allowed us to control for the depth dependence of Δ^{14}C as well as simplify interpretation of the data. In order to obtain estimates of these data for the 0-30 cm depth increment we computed carbon mass-weighted means for $\Delta^{14}C_{bulk}$ and flux-weighted means for $\Delta^{14}C_{respired}$; these calculations were made prior to determining $\Delta^{14}C_{bulk\text{-}respired}$.

Eq. 4

$$\Delta^{14}C = \alpha + \beta_1(Metal_x) + \beta_2(time) + \epsilon$$

Results

Soil carbon concentration depth profiles

We observed both parent material and climate effects on soil C concentration. Carbon concentrations were similar among parent materials for the warm climate sites (**Fig. 2, a**), while at the cool and cold climate sites (**Fig. 2, b, c**) the andesitic soils had higher C concentrations than either the basaltic or granitic soils. The basaltic and granitic soils had similar C concentrations across climate zones, while the cool and cold climate andesitic soils were enriched in C relative to the warm climate soils. Soils showed a similar decrease in C concentration with depth across all sites (**Fig. 2**).

We did not observe significant changes in soil C concentration over time at the majority of sites. However, there were a few exceptions. Most notably, we saw significant increases in soil C concentration for the cold climate andesitic soils at all depths (lower and upper 95% confidence limits given in brackets), with increases of: 0.20 [0.01, 0.40], 0.23 [0.12, 0.35], 0.21 [0.13, 0.29] percent C yr^{-1}, for the 0-10, 10-20, and 20-30 cm depth increments, respectively. We also saw a significant increase in percent C over time for the 10-20cm layer at the warm climate granitic site (0.16 [0.05, 0.26] percent C yr^{-1}), and significant decreases for the 0-10cm layer at the warm climate andesitic and basaltic sites (-0.19 [-0.37, -0.01], 0.04 [-0.07, 0.14] percent C yr^{-1}).

Radiocarbon depth profiles

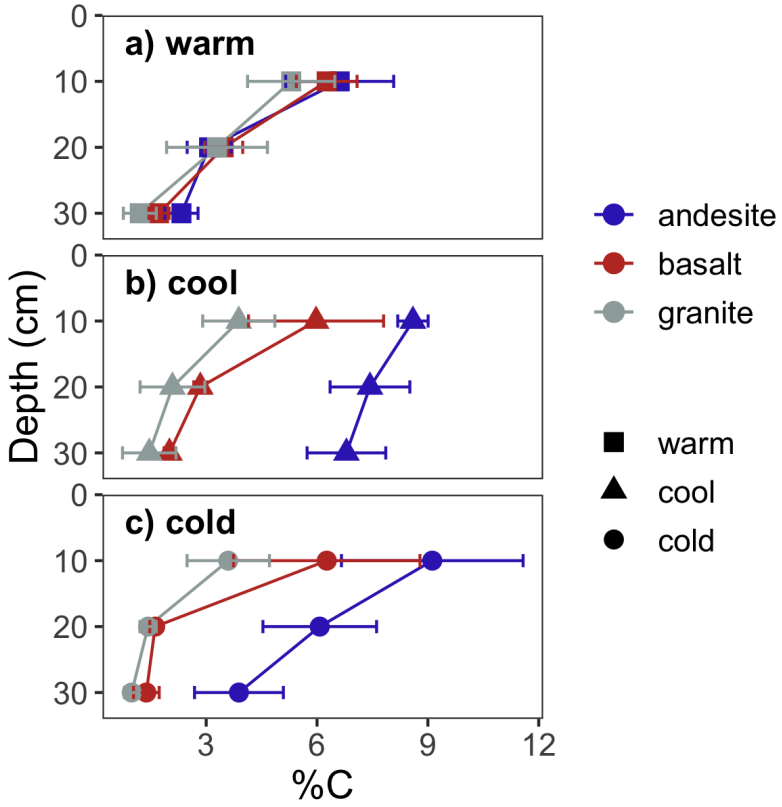

Figure 2. Profiles of soil C concentration. Points show means of 2001, 2009, and 2019 data; error bars show ±2SE.

Bulk soil. The distribution of $\Delta^{14}C_{bulk}$ showed both parent material and climate controls, as with soil C concentration. However, contrary to what would be expected from the decomposition-temperature relationship, $\Delta^{14}C_{bulk}$ of soils at the cool climate sites was equally or more depleted than what we observed at the cold climate sites (**Fig. 3, b, c**), although we observed the most enriched $\Delta^{14}C_{bulk}$ at the warm climate sites (**Fig. 3, a**). When comparing $\Delta^{14}C_{bulk}$ from different parent materials within a given climate zone, $\Delta^{14}C_{bulk}$ of andesitic soils tended to be the most depleted, while the granitic soils tended to be the most enriched (**Fig. 3**).

Analysis of variance for $\Delta^{14}C_{bulk}$ revealed significant two-way interactions between parent material and climate at all depths (**Table 1**). This interaction was evident in the

differences in $\Delta^{14}C_{bulk}$ that we observed among parent materials within a given climate zone. We observed the greatest differences in $\Delta^{14}C_{bulk}$ among parent materials at the warm and cool sites (**Fig. 3, a, b**), while $\Delta^{14}C_{bulk}$ was similar among parent materials at the coldest sites (**Fig. 3, c**). We also found depth to be an important factor influencing the relative importance of climate versus parent material effects on $\Delta^{14}C_{bulk}$. Although $\Delta^{14}C_{bulk}$ declined with depth for all sites, climate explained more of the variance in $\Delta^{14}C_{bulk}$ in the uppermost soil layer (0-10 cm) whereas parent material explained more in the bottom two layers (10-20 cm, 20-30 cm) (**Table 1**).

Heterotrophically respired CO_2. The patterns we observed in $\Delta^{14}C_{respired}$ were similar to those we observed in $\Delta^{14}C_{bulk}$ (**Fig. 3**). We found climate to be the most significant factor for explaining the variance observed in $\Delta^{14}C_{respired}$ for the uppermost soil layer, and parent material to be more important than climate for explaining in $\Delta^{14}C_{respired}$ variance at the deepest depth, as with $\Delta^{14}C_{\text{bulk}}$. However, unlike $\Delta^{14}C_{bulk}$, parent material was not significant for explaining the variance in $\Delta^{14}C_{respired}$ in the uppermost soil layer (**Table 1**). Overall, the two-way interaction between parent material and climate explained more of the variance in $\Delta^{14}C_{respired}$ data than in the $\Delta^{14}C_{bulk}$ data (**Table 1,** F **values**).

In general, the effect of climate on $\Delta^{14}C_{\text{respired}}$ appeared to be moderated by the effect of parent material. For example, we did not observe significant differences in $\Delta^{14}C_{respired}$ among the andesitic soils when compared across climate zones at any depth (SI Table X Tukey results for emm?). In contrast, $\Delta^{14}C_{respired}$ for the basaltic and granitic soils diverged substantially between climate zones, particularly for the 10-20 cm and 20-30 cm depth layers (**Fig. 3**). Overall, $\Delta^{14}C_{respired}$ across sites was most similar at the soil surface, and most divergent at the intermediate depth (10-20 cm) (**Fig. 3**).

Radiocarbon timeseries

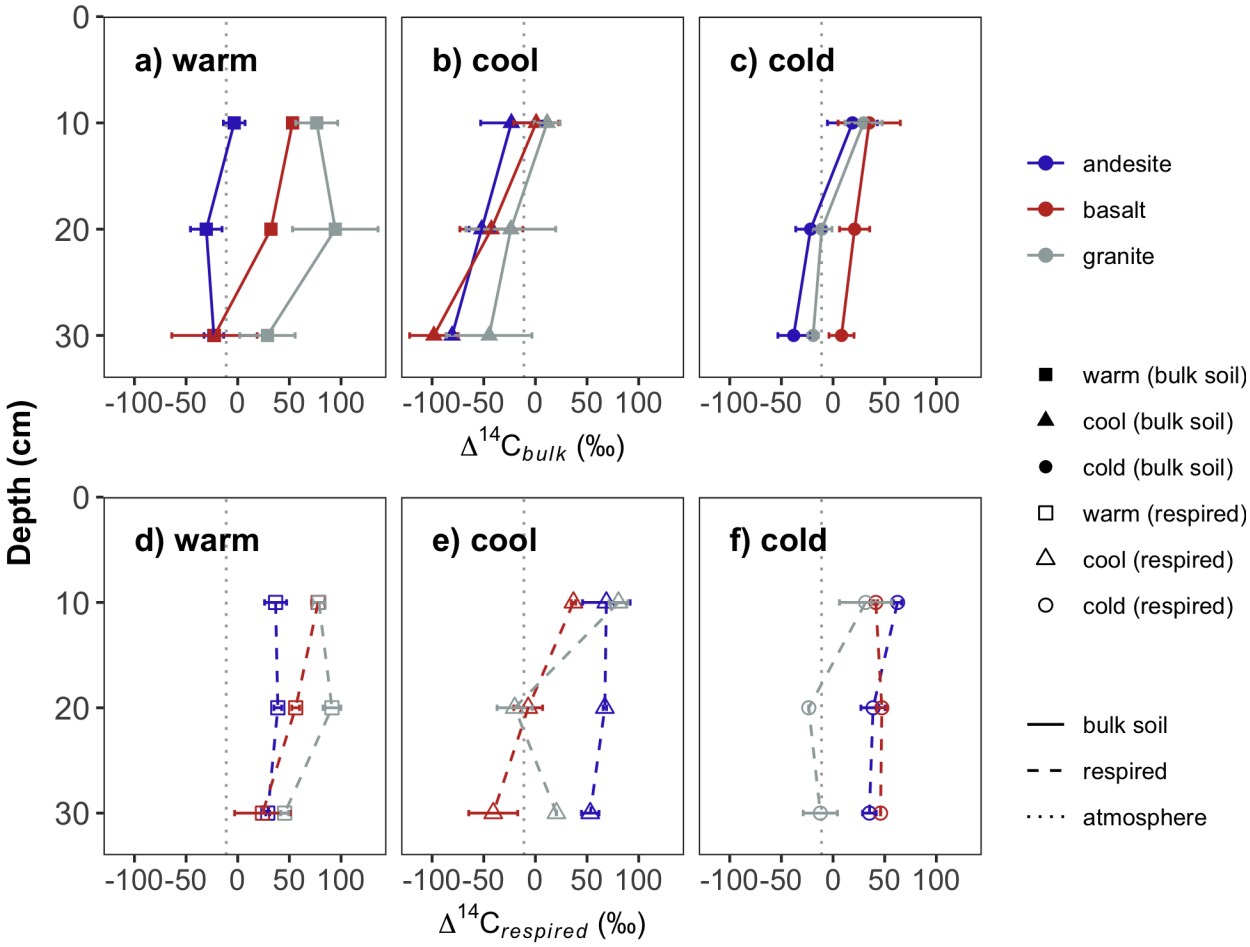

Figure 3. Depth profiles of $\Delta^{14}C_{bulk}$ and $\Delta^{14}C_{respired}$ in 2019. Top panels show bulk data, bottom panels show respired data. Panels (a) and (d) show data from the warm climate sites, (b) and (e) from the cool climate sites, and (c) and (f) from the cold climate sites. Black vertical lines show $\Delta^{14}C$ of the atmosphere in 2019. Points show the mean of three replicate profiles for bulk soil, and the mean of laboratory duplicates for respired CO_2. Error bars show ±1 SD for bulk soils and the minimum and maximum for respired CO_2.

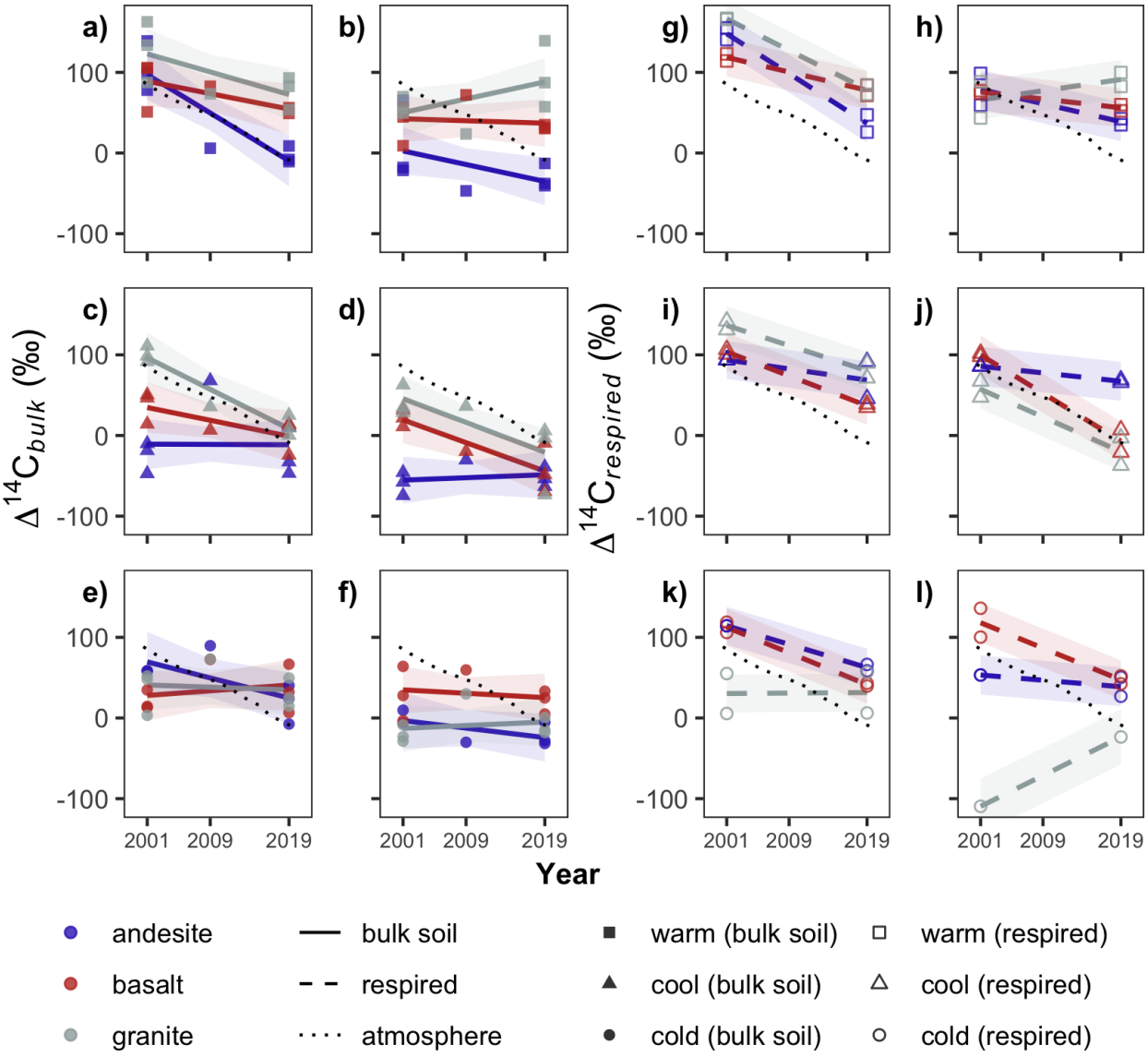

Figure 4. Temporal trends in $\Delta^{14}C$ for 0-10 cm and 10-20 cm depth layers. Panels a-f show $\Delta^{14}C_{bulk}$ data; from left, the first column (panels a, c, and e) show 0-10 cm data, and the second column (panels b, d, and f) shows 10-20 cm data. Panels g-l show $\Delta^{14}C_{respired}$ data; the third column from left (panels g, i, k) shows 0-10 cm data, and the rightmost column (panels h, j, and l) shows 10-20 cm data. Points show observed data; lines show linear trend estimates for marginal means; ribbons show 95% confidence intervals for trends. Dotted line shows atmospheric $\Delta^{14}C$.

Table 1

ANOVA for $\Delta^{14}C_{\text{bulk}}$ *and* $\Delta^{14}C_{\text{respired}}$

		Bulk soil			Respiration		
Depth	Predictor	*df*	*F*	*p*	*df*	*F*	*p*
0-10cm	Parent material	2	9.64	**< .001**	2	0.49	0.622
	Climate	2	18.63	**< .001**	2	18.34	**< .001**
	Year	1	24.85	**< .001**	1	116.25	**< .001**
	Parent material:Climate	4	3.37	**0.017**	4	12.40	**< .001**
	Parent material:Year	2	1.79	0.179	2	0.78	0.475
	Climate:Year	2	3.90	**0.028**	2	5.16	**0.017**
	Parent material:Climate:Year	4	3.15	**0.023**	4	5.98	**0.003**
	Residuals	44			18		
20-30cm	Parent material	2	20.25	**< .001**	2	7.06	**0.006**
	Climate	2	10.67	**< .001**	2	2.03	0.164
	Year	1	4.19	**0.047**	1	0.18	0.68
	Parent material:Climate	4	2.74	**0.04**	4	7.22	**0.002**
	Parent material:Year	2	3.25	**0.048**	2	11.10	**< .001**
	Climate:Year	2	9.71	**< .001**	2	7.87	**0.004**
	Parent material:Climate:Year	4	2.70	**0.043**	4	2.38	0.095
	Residuals	44			16		

Bulk soil. We observed a significant three-way interaction between parent material, climate, and time at all three depths in the linear models (**Eq. 1**) for $\Delta^{14}C_{bulk}$ (**Table 1**). The change over time in $\Delta^{14}C_{bulk}$ was also affected by depth, with greater differences between 2001 and 2019 seen in the uppermost soil layer than in the deeper layers (**Fig. 4**). We observed a significant decrease in $\Delta^{14}C_{bulk}$ in both warm and cool climate granitic soils for the uppermost soil layer, and additionally for the warm climate andesitic soils (**Fig. 4, a**). In the deeper soil layers (10-20 cm and 20-30 cm), we only observed a significant change over time in $\Delta^{14}C_{bulk}$ in the cool climate basalt and granite soils (**Fig. 4, b, c**). $\Delta^{14}C_{bulk}$ of

the cool climate andesitic soils remained essentially unchanged between 2001 and 2019 for all depths (**Fig. 4, a, b, c**), underscoring the importance of the interaction between parent material and climate for explaining temporal trends in $\Delta^{14}C_{bulk}$ as well as variance in a given year.

The relationship of $\Delta^{14}C_{bulk}$ to atmospheric $\Delta^{14}C$ also depended on the combination of parent material and climate. In 2001, the warm climate sites were the only sites where the basaltic and andesitic soils were enriched relative to the atmosphere, and this enrichment was only observed for the uppermost soil layer (**Fig. 4)**). In contrast, granitic soils at both the warm and cool granitic sites were enriched relative to the atmosphere in 2001 (**Fig. 4**). For the cold climate sites, where $\Delta^{14}C_{bulk}$ was most similar, all three lithologies were depleted relative to atmospheric in both surface and subsoil layers (**Fig. 4**).

We observed that $\Delta^{14}C_{bulk}$ tended to decrease or remain unchanged between 2001 and 2019 across sites, but the rates of change in $\Delta^{14}C_{bulk}$ were typically smaller than the corresponding change in atmospheric $\Delta^{14}C$ over the same period (-5.13 per mille yr^{-1}). Accordingly, $\Delta^{14}C_{bulk}$ measured in 2019 tended to be enriched relative to the atmosphere at more sites, and also deeper into the soil than in 2001. We observed surface soil $\Delta^{14}C_{bulk}$ (0-10 cm) in 2019 to be enriched relative to the atmosphere at all sites except for the cool climate andesite soils (**Fig. 4; Fig. 3, d-f**). Furthermore, $\Delta^{14}C_{bulk}$ remained enriched relative to the atmosphere down to 30 cm at two of the sites in 2019: the warm climate granite soil (**Fig. 3, d**) and cold climate basalt soil (**Fig. 3, f**). $\Delta^{14}C_{bulk}$ at the cool andesite site was the most depleted relative to the atmosphere at all time points (**Fig. 4**).

Heterotrophically respired CO_2. Temporal trends in $\Delta^{14}C_{respired}$ were similar to what we observed for $\Delta^{14}C_{bulk}$, but tended to be of greater magnitude (**Fig. 4, g-l**). Although greater than the change over time we observed in $\Delta^{14}C_{bulk}$, changes in $\Delta^{14}C_{respired}$ between 2001 and 2019 still tended to be smaller in magnitude than the change observed in the atmosphere over this period (**Fig. 4, g-l**). In contrast to $\Delta^{14}C_{bulk}$, $\Delta^{14}C_{respired}$ tended to

be indistinguishable or enriched relative to the atmosphere in both 2001 and 2019; while the majority of samples were enriched relative to the atmosphere in 2019, even at depth (**Fig. 4, g-l**).

We saw significant decreases in surface soil $\Delta^{14}C_{respired}$ at seven of the nine sites, with the only exceptions being the cool andesitic and cold granitic sites (**Fig. 4, i, k**). In absolute terms, the changes in $\Delta^{14}C_{respired}$ over time in these uppermost soil layers were greatest at the warm sites (-4.4 per mil ± 2 yr^{-1}), while changes were similar for the cool and cold sites (-2.7 per mil ± 1.2 yr^{-1}, and -2.3 per mil ± 2.1 yr^{-1}, respectively). When considered within parent materials, granitic soils showed greatest decreases $\Delta^{14}C_{respired}$ over time at the warm climate sites and the least change at the cold climate sites. In contrast, the andesitic soils showed the least amount of change over time at the cool climate sites, while there were no significant differences among climate zones for the basaltic soils. The magnitude of the change in $\Delta^{14}C_{respired}$ over time tended to decrease with depth for all soils. We observed significant negative trends over time for $\Delta^{14}C_{respired}$ at only four of the nine sites for the 10-20 cm layer (warm andesite, cool basalt, cool granite, and cold basalt) (**Fig. 4**), and only one site for the 20-30 cm layer (cold basalt) (SI). $\Delta^{14}C_{respired}$ at the cool andesitic soils remained unchanged at all depths over the study period.

We observed a significant increase in $\Delta^{14}C_{respired}$ from 2001 to 2019 at only one site: from the cold climate granitic soils (**Fig. 4**). These were also the only soils for which $\Delta^{14}C_{respired}$ was more depleted than $\Delta^{14}C_{bulk}$. We observed this anomaly for the deeper soil layers in both 2001 and 2019. For the 8-27 cm layer in 2001, the range of $\Delta^{14}C_{respired}$ values was -469.10 and -127.80 per mil, compared to a range of $\Delta^{14}C_{bulk}$ values of -30.80 and -10.50; similarly, for the 10-20 cm layer in 2019 we observed a range of $\Delta^{14}C_{respired}$ values of -396.70 and -23.50 per mil compared to -18.10 and 0.40 for $\Delta^{14}C_{bulk}$ (SI Table X). We do not believe this was due to laboratory error in spite of the high variance we observed in the samples, as the pattern was restricted to the deeper soil layers from this one site and consistent over

time. However, since it appears to be a unique response to these soils, we have excluded these highly depleted samples from the statistical analyses.

Relationship of bulk soil and respired CO_2 $\Delta^{14}C$

We also assessed whether interaction effects of parent material or climate with $\Delta^{14}C_{bulk}$ led to deviations from a 1:1 relationship with $\Delta^{14}C_{respired}$ (**Fig. 5**). We found that changes in $\Delta^{14}C_{bulk}$ led to correspondingly smaller changes in $\Delta^{14}C_{respired}$ for andesitic soils in the parent material only model (**Eq. 2**) (slope = 0.51, 95% CI = [0.22, 0.80]) (**Fig. 5, a**), and for cool climate soils in the climate only model (**Eq. 3**) (slope = 0.61, 95% CI = [0.30, 0.91]) (**Fig. 5, b**). While we could not directly test the interaction of parent material and climate factors in these models owing to the limited number of observations, mean differences in $\Delta^{14}C_{bulk}$ and $\Delta^{14}C_{respired}$ were substantially greater for the cool climate soils developed on andesitic parent material than for the other sites (Table? Numbers?).

Mineral assemblages and radiocarbon

Mineral assemblage data is reported fully in Rasmussen et al. (2018). Here we focus on the selective dissolution data with respect to the trends we observed in $\Delta^{14}C_{bulk}$, $\Delta^{14}C_{respired}$, and $\Delta^{14}C_{respired\text{-}bulk}$. We observed a significant negative correlation between $\Delta^{14}C_{bulk}$ and the concentration of oxalate extractable iron, oxalate extractable aluminum, and pyrophosphate extractable aluminum (SI). For simplicity, we focus here on the sum of oxalate extractable aluminum and half of the oxalate extractable iron as a proxy for poorly crystalline mineral abundance, and the difference of dithionite-citrate extractable iron and ammonium-oxalate extractable iron as a proxy for crystalline mineral abundance. The relationship between non-crystalline mineral abundance and $\Delta^{14}C_{bulk}$ was highly significant (p <0.001), with the model explaining 59 percent of the observed variation. In contrast, we did not find a significant relationship between crystalline mineral abundance and $\Delta^{14}C_{bulk}$.

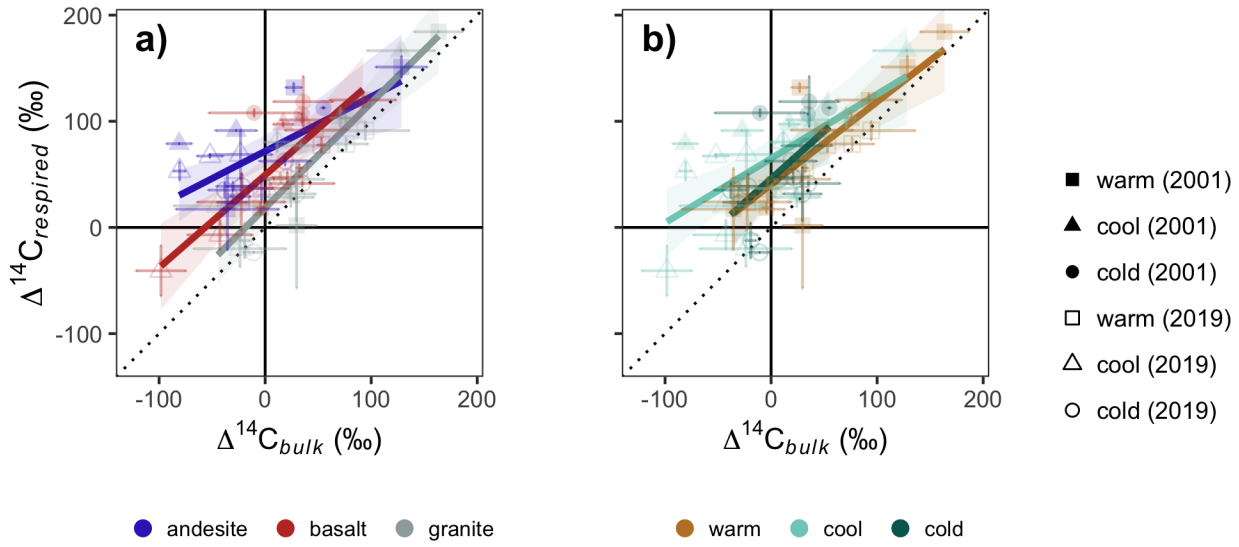

Figure 5. Parent material and climate effects on the relationship of $\Delta^{14}C_{bulk}$ and $\Delta^{14}C_{respired}$. [a)] Parent material model **(Eq. 3)** and [b)] Climate model **(Eq. 4)**. Dotted line shows 1:1 relationship. Points show the mean of three replicate profiles for bulk soil, and the mean of laboratory duplicates for respired CO_2. Error bars show ±1 SD for bulk soils and the minimum and maximum for respired CO_2. Respired CO_2 from the cold granite site in 2001 was extremely depleted in $\Delta^{14}C$ and thus is excluded for display purposes.

We also observed a significant ($p = 0.02$) negative relationship between $\Delta^{14}C_{respired}$ and non-crystalline mineral abundance, although it was not as strong as the $\Delta^{14}C_{bulk}$ relationship. However, we observed a stronger relationship between poorly crystalline mineral abundance and $\Delta^{14}C_{respired\text{-}bulk}$ (**Fig. 6, a**) than for either $\Delta^{14}C_{bulk}$ or $\Delta^{14}C_{respired}$. As with $\Delta^{14}C_{bulk}$, there was no relationship with crystalline mineral abundance for either $\Delta^{14}C_{bulk}$ or $\Delta^{14}C_{respired\text{-}bulk}$ (**Fig. 6, b**).

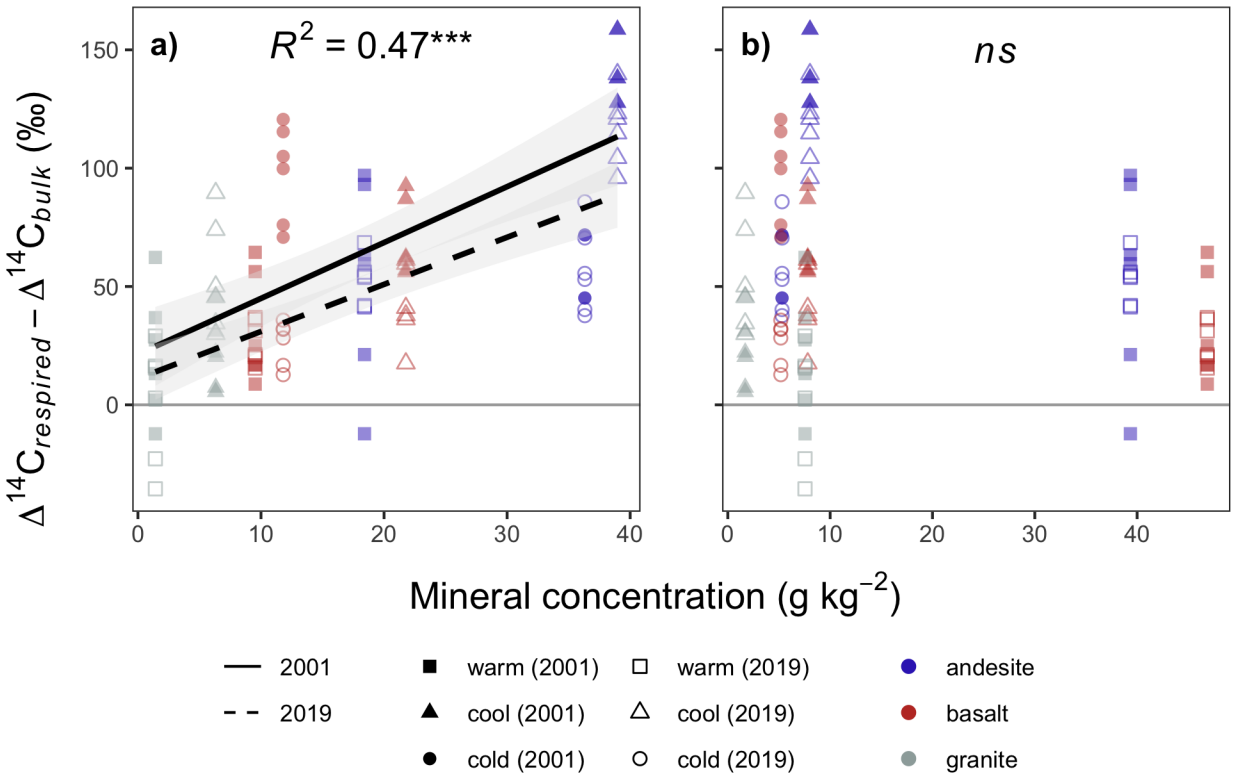

Figure 6. Relationship of poorly crystalline and crystalline minerals to the difference of $\Delta^{14}C_{respired}$ and $\Delta^{14}C_{bulk}$ ($\Delta^{14}C_{respired\text{-}bulk}$). [a)] Poorly crystalline mineral content (oxalate-extractable aluminum + 1/2 oxalate-extractable iron), [b)] Crystalline mineral content (dithionite-extractable iron - oxalate-extractable iron). Points show mass-weighted mineral concentrations and carbon-weighted values of $\Delta^{14}C_{respired\text{-}bulk}$ for 0-30cm profiles. Lines show linear model fits from **Eq. 5**.

Discussion

In this study we considered the relative effects of parent material and climate on the distribution of radiocarbon in bulk soils and heterotrophically respired CO_2 in order to determine how these factors control the cycling of soil C across timescales of years to centuries. Our key finding is that the patterns we observed in both $\Delta^{14}C_{bulk}$ and $\Delta^{14}C_{respired}$ could only be explained by considering the interaction of parent material and climate in addition to the effects of each factor alone. Furthermore, we found that we could explain this interaction quantitatively through the abundance of poorly crystalline minerals, which both form and are preferentially retained at sites with soils in intermediate stages of weathering.

We found evidence for the overarching effects of climate on decomposition with respect to increases in both soil C concentration and the apparent age of soil C (by proxy from $\Delta^{14}C_{bulk}$) with decreasing temperature. However, the increase in soil C concentration with temperature was not linear, with substantially less C observed in the warm climate sites than in the cool climate sites, but similar soil C concentrations observed at the cool and cold climate sites. Furthermore, we observed the most depleted $\Delta^{14}C_{bulk}$ at the cool climate sites, rather than at the cold climate sites. These results suggest that there is a mechanism at work in the cool climate zone soils that is slowing soil C decomposition and leading to correspondingly greater rates of soil C accumulation, and increased soil C persistence, than would otherwise be predicted on the basis of temperature alone.

We also observed differences in both soil C concentration and soil radiocarbon values due to parent material. The effect of parent material on soil C concentration was most pronounced at the cool and cold climate sites, while the effect on soil radiocarbon was most evident at the warm and cool climate sites. Overall, the andesitic soils were the most enriched in soil C and tended to have the most depleted values of $\Delta^{14}C_{bulk}$ The granite soils tended to have the lowest soil C concentrations and $\Delta^{14}C_{bulk}$ values that were the most

enriched, while the basalt soils were intermediate between the granite and andesitic soils with respect to both soil C concentration and $\Delta^{14}C_{bulk}$ These findings highlight the importance of the primary mineral composition of a soil in determining both soil carbon accumulation and persistence.

Parent material is an important determinant of soil mineral assemblages, but the mineral make-up of a soil changes over time due to weathering. Rasmussen (2004) observed that mineral assemblages were the most similar among the three different parent materials in the highly weathered soils of the warm climate sites. These sites were also where we saw the least amount of differences in soil C concentration in the present study. In contrast, Rasmusssen (2004) observed the greatest differences in mineral assemblages at the cool climate sites, which is where we also saw the strongest divergence from the expected relationship between temperature and soil C dynamics. These findings provide evidence to support the important role played by specific soil minerals in explaining the highly significant interaction of parent material and climate we observed in this study.

Our results point to poorly crystalline minerals as the key to explaining both soil C accumulation and persistence in soils. In contrast, the lack of correlation we observed between crystalline minerals and soil radiocarbon suggests that these minerals do not play an important role in explaining soil C persistence, at least in these soils. Other studies have shown that crystalline minerals do protect soil C from microbial decomposition, but that the overall sorption capacity of these mineral species is low. We observed a large increase in the amount of iron dissolved from crystalline minerals at the warm sites, relative to the cool or cold sites, along with a corresponding decrease in soil C concentration and relative enrichment in both $\Delta^{14}C_{bulk}$ and $\Delta^{14}C_{respired}$. Furthermore, this increase in crystalline iron was also associated with a corresponding decrease in the amount of poorly crystalline minerals. Together these trends suggest that these soils have lost poorly crystalline minerals through weathering, via leaching and transformation into crystalline species, with negative

consequences for soil carbon storage.

The importance of poorly crystalline minerals for explaining trends in soil carbon persistence is well documented (cite). We corroborate those findings in this study with strong negative correlation observed between bulk soil radiocarbon and poorly crystalline mineral content. Accordingly, we observed the most depleted $\Delta^{14}C_{bulk}$ in the cool climate andesitic soils, where poorly crystalline mineral content was also the highest. We also observed an equally strong correlation between poorly crystalline mineral content and the difference between $\Delta^{14}C_{respired}$ and $\Delta^{14}C_{bulk}$ Again, this difference was greatest for the cool climate andesitic soils. These correlations suggest that associations between soil organic matter and poorly crystalline minerals actively inhibit decomposition even under the favorable incubation conditions provided in the laboratory. If true, this protective effect would also allow for long-term soil C persistence *in situ*.

Mineral-association is known to play an important role in the regulation of long-term soil organic matter persistence. However, our data indicate that poorly crystalline mineral content is also associated with the presence of a decadally cycling soil C pool. We observed $\Delta^{14}C_{respired}$ at the cool climate andesitic site to be enriched relative to the atmosphere in both 2001 and 2019, and additionally, we did not detect any substantial change in $\Delta^{14}C_{respired}$ at this site over time. This indicates that these soils are respiring decadally cycling soil C enriched with bomb-C. We suggest that the presence of this decadally cycling C in conjunction with a pool of much older soil C, as evinced from the $\Delta^{14}C_{bulk}$ data, implies that there is a range of timescales of mineral-associated soil C persistence, encompassing annual to decadal scales as well as centennial to millennial.

We measured both $\Delta^{14}C_{respired}$ and $\Delta^{14}C_{bulk}$ in this study to assess the relative accessibility of soil organic matter to decomposition among soils where we expected to find different degrees of mineral mediated soil C persistence. The presence of protected pools of soil organic matter leads to differences between these radiocarbon signals, whereas the

absence of protection mechanisms results in similar values for $\Delta^{14}C_{respired}$ and $\Delta^{14}C_{bulk}$. We observed the smallest differences between $\Delta^{14}C_{respired}$ and $\Delta^{14}C_{bulk}$ for the soils developed on granitic parent material. The mineral assemblages in these soils are dominated by phyllosilicates, providing evidence that the association between soil organic matter and these minerals does not provide substantial protection against microbial decomposition. Carbon in these soils was still depleted relative to the atmosphere at depth, but the similarity between $\Delta^{14}C_{respired}$ and $\Delta^{14}C_{bulk}$ in these soils suggests that soil C persistence in these soils is due to decomposition constraints that are alleviated under laboratory incubation conditions.

The sensitivity of decomposition to temperature is of particular interest for understanding how soil C dynamics may change under a warming climate. We sought to assess the role of mineral association in attenuating this temperature sensitivity by comparing the changes observed in $\Delta^{14}C_{respired}$ over time at the soil surface, where climate effects were strongest. We did not see any significant differences in the magnitude of the change in $\Delta^{14}C_{respired}$ over time due to climate for the basalt soils. In contrast, the granite soils showed the most change in the warmest climate and the least change in the coldest climate, as would be expected from purely thermodynamic control over decomposition; and the andesitic soils showed the least change in the coolest climate site, as would be expected if mineral association decreased the temperature sensitivity of decomposition.

Conclusion

Our study shows clearly that parent material and climate interact to control soil C dynamics. This interaction was the key to explaining trends in $\Delta^{14}C_{bulk}$, which is a proxy for the mean age of soil C, and additionally in $\Delta^{14}C_{respired}$, which reveals the relative contributions of faster or more slowly cycling soil C to respiration. We observed that the trends in both $\Delta^{14}C_{bulk}$ and $\Delta^{14}C_{respired}$ were best explained by climate at the soil surface, but best explained by parent material in deeper soil layers. This importance of climate was

reflected in the changes in $\Delta^{14}C$ (both bulk and respired) we observed over time, which were greater for surface soils than deeper soils, and greater for the highly weathered soils at the warm sites than the poorly developed soils at the cold sites. Yet contrary to the expected temperature-decomposition relationship, we saw the most depleted $\Delta^{14}C_{bulk}$ in the cool climate andesitic soil, which is also where we saw the least change over time at all depths.

The effect of the interaction between parent material and climate on soil C dynamics is best explained by the development of distinct mineral assemblages via weathering, in particular the formation and subsequent loss of poorly crystalline secondary minerals. We confirm the findings of other studies that poorly crystalline minerals are highly correlated with the age of soil C, as measured by proxy with $\Delta^{14}C_{bulk}$. We extend this finding to show that it is specifically the poorly crystalline mineral content that is correlated with $\Delta^{14}C_{bulk}$, while crystalline mineral content is not. Furthermore, we provide mechanistic evidence for the protective effect of mineral-association on decomposition of soil organic matter by demonstrating that the difference between $\Delta^{14}C_{bulk}$ and $\Delta^{14}C_{respired}$ is even more strongly correlated with poorly crystalline mineral content than $\Delta^{14}C_{bulk}$ alone. In conclusion, we posit that that the association of soil organic matter with poorly crystalline minerals may attenuate the temperature sensitivity of decomposition, and that this dampening effect should be considered in the next generation of soil C models.

In future work we intend to quantify the timescales of soil carbon cycling in mineral and non-mineral associated pools with a compartmental modeling approach, using the radiocarbon time series presented here in addition to radiocarbon measurements of soil density and thermal fractions as constraints. With this modeling framework we also hope to explore hypotheses regarding mineral association and temperature sensitivity further.